

POTENTIALLY HAZARDOUS ELEMENTS IN ATMOSPHERIC PRECIPITATION DURING THE WARM SEASON (MAY–SEPTEMBER) OF 2019 IN MOSCOW

Dmitrii Vlasov^{1*}, Irina D. Eremina², Natalia E. Kosheleva³, Galina Shinkareva^{1,4},
Natalia E. Chubarova², Nikolay S. Kasimov³

¹ Department of Geography, Geology, and the Environment, Illinois State University, IL 61790, Normal, USA

² Department of Meteorology and Climatology, Faculty of Geography, Lomonosov Moscow State University, 119991, Moscow, Russian Federation

³ Department of Landscape Geochemistry and Soil Geography, Faculty of Geography, Lomonosov Moscow State University, 119991, Moscow, Russian Federation

⁴ Department of Geosciences, Middle Tennessee State University, TN 37132, Murfreesboro, USA

*Corresponding author: vlasov.msu@gmail.com

Received: May 21st 2024 / Accepted: July 25th 2024 / Published: October 1st 2024

<https://doi.org/10.24057/2071-9388-2024-3408>

ABSTRACT. Atmospheric precipitation acts as a significant pathway for pollutants from the atmosphere to the Earth's surface, and analyzing urban precipitation data on intensity, fallout regime, transfer patterns, and solid particle content helps identify pollution sources. For the first time in the Moscow megacity, the levels of soluble forms of potentially hazardous elements (PHEs) in atmospheric precipitation were studied during the whole summer season of May–September 2019. The concentrations of Al, As, B, Ba, Be, Bi, Cd, Ce, Co, Cu, Fe, La, Li, Mn, Ni, P, Pb, Rb, Sb, Sn, Sr, and Zn were determined using inductively coupled plasma mass spectrometry and atomic emission spectroscopy methods. The research underscores the crucial role of atmospheric precipitation in washing PHEs out of the atmosphere. In May and September, concentrations of PHEs surpass the warm-season average. Notable contamination in May stems from elevated traffic during vacations, extensive burning of plant debris and wood, and pollen transport. Summer months are characterized by reduced forest and agricultural fires, traffic, and increased vegetation, leading to lower PHE concentrations, especially in July, with typical amount of precipitation contributing to pollutant dispersion. Elevated PHE levels in September are observed due to increased traffic load, biomass burning, and the expansion of unvegetated soil areas. Rainwater is enriched with Sb, Pb, Cd, Zn, Cu, B, Bi, P, and Sr, sourced from vehicle emissions, soil particles, industry, construction dust, biomass burning, and forest fires. Moderate enrichment with Ba, Mn, Ni, Co, and Sn also occurs episodically. Regression analysis highlights solid particles' role as a major PHE source in rainwater, with the longer antecedent dry periods and the higher acidity level of rain intensifying the accumulation of PHEs. Long-range transport plays a lesser role, with Southern and Northern Europe, Western Siberia, and the central part of European Russia contributing meaningfully.

KEYWORDS: rainwater, metals and metalloids, urban environment, sources of contamination, atmospheric pollution, anthropogenic impact

CITATION: Vlasov D., Eremina I. D., Kosheleva N. E., Shinkareva G., Chubarova N. E., Kasimov N. S. (2024). Potentially Hazardous Elements In Atmospheric Precipitation During The Warm Season (May–September) of 2019 In Moscow. *Geography, Environment, Sustainability*, 3(17), 70-84
<https://doi.org/10.24057/2071-9388-2024-3408>

ACKNOWLEDGEMENTS: The study was supported by the Russian Science Foundation (grant № 19–77–30004–P).

Conflict of interests: The authors reported no potential conflict of interest.

INTRODUCTION

Atmospheric precipitation plays a crucial role in the global hydrogeochemical cycle (Seinfeld and Pandis 2016; Bezrukova and Chernokulsky 2023), acting as a significant pathway for transporting atmospheric pollutants to the Earth's surface (Zeng et al. 2024a). Observations of atmospheric parameters and the chemical composition of precipitation in urban areas yield valuable insights into both local and remote sources of pollution, which determine the levels of heavy metals, metalloids, and other

toxic elements and compounds present in rainwater. Joint analysis of the data, including factors such as precipitation intensity, duration of preceding dry periods, long-range transport patterns, atmospheric dust levels, etc., facilitates the identification of weather conditions leading to the highest levels of contamination in precipitation with toxic elements and compounds, as well as assessing the frequency of such events (Vlasov et al. 2021a, 2021b; Adhikari et al. 2023; Rathore et al. 2023; Zeng et al. 2024b).

Analyzing the chemical composition of atmospheric precipitation allows for the assessment of the intensity

of washing out and deposition of potentially hazardous elements (PHEs), including carcinogens such as As, Cd, Pb, Be, Ni, and Co, as well as those causing systemic toxicity to the body or specific organs and systems, such as Sb, Zn, Cu, Sn, Ba, Mn, and others (Bayramoğlu Karşı et al. 2018; Orlović-Leko et al. 2020; Tsamos et al. 2022). Therefore, PHE content in atmospheric precipitation has been extensively studied worldwide. In Russia, such studies are often conducted in background areas, while the analysis of PHEs in urban precipitation is less frequent (Chudaeva et al. 2008; Yanchenko and Yaskina 2014; Semenets et al. 2017; Stepanets et al. 2021; Bezrukova and Chernokulsky 2023). In Moscow, the largest megacity in Europe, the content of organic compounds in individual rain samples has been analyzed (Polyakova et al. 2018), the ratio of PHE forms in spring precipitation in 2018 and 2019 has been determined (Chubarova et al. 2020; Vlasov et al. 2021a, 2021b), and the role of precipitation in the purification of the atmosphere from metals and metalloids accumulated in aerosols in April–July 2020 was assessed (Kasimov et al. 2023). However, the content of PHEs in precipitation and its variability throughout the entire warm period (May–September) in Moscow megacity has not been studied in detail.

Therefore, the study aims to examine the distribution of PHEs in atmospheric precipitation in Moscow during the entire warm period, when the influence of heating-related pollution is less pronounced compared to the increased contribution from other sources: vehicular traffic, industrial enterprises of various sectors, soil and road dust particle resuspension, forest and agricultural fires in the Moscow region, controlled burning of biomass and waste, etc. Data from measurements conducted at the Meteorological Observatory of Lomonosov Moscow State University (MO MSU) were used.

We focused on solving the following problems: (1) to determine the content of PHEs and its variability in atmospheric precipitation during the studied period based on observation data; (2) to identify the main sources of PHEs; and (3) to analyze the influence of the precipitation amount and the properties of rainwater, as well as air advection regions, on the content of PHEs in precipitation.

MATERIALS AND METHODS

The Meteorological Observatory of Lomonosov Moscow State University (55.707° N, 37.522° E) is located in the MSU Botanical Garden, far from local industrial pollution sources and highways; and can be considered a background city site (Chubarova et al. 2024). For characterizing meteorological conditions during the analyzed period, we used standard meteorological measurements and compared them with monthly means over 60 years of observations since 1954 (Chubarova et al. 2014).

Precipitation samples (N=56) were taken at a height of 2 m from the ground surface using a vinyl plastic funnel (80×80 cm) and a white plastic bucket. Each case of rainfall was considered from the beginning to its end on the current or adjacent days separately: there were 11 cases in May (May 2, 3, 5, 8, 9, 10, 13, 15, 16, 23, and 30), 8 cases in June (8, 14, 22, 26, 27, 28, 29, 30), 14 cases in July (2, 3, 6, 11, 12, 13–14, 16, 17, 18, 19, 20, 24, 25, 31), 12 cases in August (2, 3, 4, 5, 7, 9, 10, 15, 16, 17, 18, 19), and 11 cases in September (5, 14, 15, 16, 17, 18, 20, 22, 24, 29, 30).

In precipitation samples, pH and specific conductivity (EC, $\mu\text{S}/\text{cm}$) were determined using potentiometric and conductometric methods, respectively. To isolate soluble forms of PHEs, samples were filtered through Millipore®

filters with pore diameters of 0.45 μm . The filters were weighed on an analytical balance “Discovery DV114C” (Ohaus, Greifensee, Switzerland; repeatability: 0.1 mg) before and after filtration (with preliminary drying) to determine the mass of suspended matter on them and, accordingly, the content of solid particles in precipitation samples.

The concentrations of Al, As, B, Ba, Be, Bi, Cd, Ce, Co, Cu, Fe, La, Li, Mn, Ni, P, Pb, Rb, Sb, Sn, Sr, and Zn in the resulting solution were determined at the N.M. Fedorovskiy VIMS laboratory using inductively coupled plasma mass spectrometry (ICP-MS) and inductively coupled plasma atomic emission spectroscopy (ICP-AES) on the “iCAP Qc” mass spectrometer (Thermo Scientific, USA, produced in 2017) and “Optima–4300 DV” atomic emission spectrometer (Perkin Elmer, USA, produced in 2018) according to certified methods (NSAM № 520 AES/MS 2017). The VIMS laboratory is accredited by the Analytics International Accreditation System (AAS.A.00255) and the national accreditation system (RA.RU.21GP11); it meets the requirements of the International Standards ISO Guide 34:2009, ISO/IEC 17025:2017, and ISO/IEC 17043:2010. The VIMS laboratory is also accredited to certificate measurement techniques and provides metrological examinations in the Russian Federation (accreditation certificate No. 01.00115-2013). Standard reference materials “Trace metals in Drinking Water (TMDW)” (High-Purity Standards, USA) and blank samples were utilized. The limit of detection (LOD) for PHEs were as follows ($\mu\text{g}/\text{L}$): Al, 0.78; As, 0.066; B, 0.043; Ba, 0.021; Be, 0.002; Bi, 0.004; Cd, 0.003; Ce, 0.003; Co, 0.009; Cu, 0.16; Fe, 6.6; La, 0.0015; Li, 0.004; Mn, 0.07; Ni, 0.054; P, 10; Pb, 0.038; Rb, 0.011; Sb, 0.04; Sn, 0.012; Sr, 0.027; Zn, 0.32. For low concentrations of PHEs (<5 LOD), the relative standard deviation did not exceed 20%, and for higher concentrations of PHEs (>5 LOD), the relative standard deviation did not exceed 10%.

Due to the substantial variability of soluble PHE concentrations in precipitation from one episode to another, volume-weighted concentrations were calculated to compare individual months and periods (Eq. (1)):

$$C_w = \left(\sum (C_i \times X_i) \right) / X_s \quad (1)$$

where C_i and X_i are PHE concentration ($\mu\text{g}/\text{L}$) and the precipitation amount (mm) in the i -th episode of precipitation, X_s is the precipitation amount for the averaging period, i.e., for the entire studied warm season or for a separate month (mm).

One of the most common methods, known for its simplicity and efficiency, was chosen to identify sources of PHEs in atmospheric precipitation. It involves calculating the enrichment factors (EF) (Eq. (2)):

$$EF = \left(C_i / C_{Al} \right) / \left(K_i / K_{Al} \right) \quad (2)$$

where C_i and C_{Al} are the concentrations of the i -th and reference (Al) elements in the precipitation sample, and K_i and K_{Al} are the abundances of the i -th and reference elements in the upper continental crust. We used the crustal abundances provided by R.L. Rudnick and S. Gao (2014), $\mu\text{g}/\text{g}$: Al, 81,505; As, 4.8; B, 17; Ba, 624; Be, 2.1; Bi, 0.16; Cd, 0.09; Ce, 63; Co, 17.3; Cu, 28; Fe, 39,180; La, 31; Li, 21; Mn, 774; Ni, 47; P, 655; Pb, 17; Rb, 84; Sb, 0.4; Sn, 2.1; Sr, 320; Zn, 67. Aluminum was used as the reference element, as in most other studies of precipitation composition in cities around the world (Özsoy and Örnektekin 2009; Guo et al. 2014; Cable and Deng 2018; Xu et al. 2022; Adhikari et al. 2023). It is considered that $EF < 10$ for soluble PHEs

indicates their natural sources (predominantly derived from the continental crust). If EF falls within the range of 10–100, anthropogenic sources are likely present, and when $EF \geq 100$, PHEs have anthropogenic sources (Chon et al. 2015).

To assess the difference in PHE content in rainwater from episode to episode, the geochemical range (GD) was calculated (Eq. (3)):

$$GD = (C_{max} / C_{min}) \quad (3)$$

where C_{max} and C_{min} are the maximum and minimum concentrations of the same PHE in the precipitation sample for the entire study period, respectively.

For comparison of dissolved PHE concentrations across different months, a "growth index" Ks was calculated (Eq. (4)):

$$Ks = (C_{w_m} / C_{w_{ave}}) \quad (4)$$

where C_{w_m} and $C_{w_{ave}}$ are the volume-weighted concentrations of a chemical element in the respective month and over the entire study period (May–September), respectively.

For a comprehensive assessment of each rainfall episode in terms of the level of all studied PHEs simultaneously, normalization was conducted (Eq. (5)):

$$C' = (C_i - C_{min}) / (C_{max} - C_{min}) \quad (5)$$

where C_i and C'_i are the original and normalized concentrations of PHEs in the i -th rainfall episode, respectively, and C_{max} and C_{min} are the maximum and minimum concentrations of PHEs over the entire warm period, respectively. Then, the total normalized concentrations of PHEs (NM) in the i -th rainfall episode can be determined as follows (Eq. (6)):

$$NM = \sum C'_{ij} \quad (6)$$

where j represents all considered PHEs (in our case, $j=1, 2, 3, \dots, 20, 21, 22$).

Descriptive statistics and correlation analysis were carried out using the Statistica 10 software by routine methods. Multivariate regression analysis was conducted to investigate the factors influencing PHE concentration in atmospheric precipitation using the method of regression (decision) trees with dendrogram construction in the SPLUS software (Kosheleva et al. 2015, 2023).

To identify possible regions of air mass advections for each rain sampling date, backward trajectories were constructed using the HYSPLIT transport–dispersion model

(Stein et al. 2015; Rolph et al. 2017), available on the READY website¹. The modeling was conducted for heights of 500, 1000, and 1500 m above ground level, with a time interval of 96 hours from 3 pm Moscow time (12 pm UTC) on the precipitation event date.

RESULTS AND DISCUSSION

Meteorological conditions during May–September, 2019

May–September 2019 was marked by variable weather conditions, significantly affecting Moscow's air pollution. Monthly mean values of the main meteorological parameters in comparison with long-term observations are shown in Table 1. One can see specific conditions in May 2019, when air temperature, water vapor pressure, and precipitation were significantly higher due to the prevailing advection of warm, humid air masses. During this month, the mineralization of precipitation was also very high compared to the 1981–2013 means (Table 1). June was characterized by an increase in air temperature by 16% and a decrease in precipitation by 10% compared to the 1954–2013 means. This happened due to the prevalence of anticyclone conditions, which can also be seen in positive atmospheric pressure deviations. The mineralization of precipitation during this month was close to the 1981–2013 mean. The situation changed in July, when due to the high frequency of cyclones over Moscow the air temperature was lower, the precipitation level was close to the norm, and the mineralization of precipitable water decreased by 22% compared to the 1981–2013 mean. In contrast, August and September had less precipitation, which changed the total mineralization of precipitable water. Compared to the averages from 1981 to 2013, mineralization was 14% lower in August and 54% higher in September. On average, the warm period of 2019 was characterized by a higher temperature (5%), lower precipitation (–19%), and higher mineralization of precipitation (16%).

Levels of PHEs and their variability in the warm season

The series of PHEs in descending order of average concentrations in precipitation at the MO MSU in the warm season is shown in Fig. 1, where the minimum and maximum concentrations of each PHE, the median, and the 25% and 75% quartiles are also indicated. The highest concentrations in precipitation are characteristic of the macroelements Fe, Al, and Pb. In terms of content levels in

Table 1. Main meteorological parameters during the warm period of 2019 at the Meteorological Observatory of Lomonosov Moscow State University² and their deviations from the monthly mean values over the 60-year period of measurements (Chubarova et al. 2014)

Period	Air temperature, deg. C		Water vapor pressure, hPa		Atmospheric pressure, hPa		Precipitation, mm		Mineralization, mg/L	
	T	deviation, %	e	deviation, %	P	deviation, %	X	deviation, %	M	deviation, %
May	16.4	23%	11.3	23%	990.9	–0.2%	64.0	17%	32.5	51%
June	19.8	16%	13.2	5%	994.6	0.5%	68.7	–10%	17.1	–3%
July	16.6	–13%	13.7	–7%	984.8	–0.5%	79.6	–2%	11.9	–22%
August	16.4	–4%	13.6	–2%	992.2	0.1%	52.9	–32%	14.0	–14%
September	12.5	10%	10.8	4%	992.1	0.0%	22.1	–65%	24.7	54%
May–September	16.3	5%	12.5	3%	990.9	0%	57.5	–19%	20.0	16%

¹ <http://www.arl.noaa.gov/HYSPLIT.php>

² www.momsu.ru

rainwater, other elements form the following descending sequence: $P > Zn > Ba > Sr > Mn > Cu > Sb > B > Ni > Rb > Co > Li > Cd > Ce > As > La > Sn > Bi$. Deviation from the order of elements by decreasing concentrations in precipitation compared to the order of elements in the continental crust is typical for Pb, Zn, Cu, Sb, Cd, and As, which is associated with the anthropogenic supply of these PHEs (Vlasov et al. 2023a; Kasimov et al. 2024).

Variations in precipitation amounts, coupled with changes in the intensity of PHE inputs into the atmosphere from natural and anthropogenic sources, result in significant differences in PHE content in rainwater in Moscow from episode to episode, which is generally typical for other cities worldwide. These differences are characterized by the geochemical range (*GD*). In warm-season precipitation in Moscow, the highest *GD* is observed for Sb (714), followed by lower values for Sr (320) and P (252). *GD* ranges from 107 to 123 for Ba, Al, and Ce, from 80 to 95 for La, Mn, and Co, decreasing to 43–56 for Pb, Rb, Li, Bi, B, and Cd, to 29–36 for Fe, Be, Ni, and Cu, to 20–22 for Sn and Zn, and to 12 for As throughout the study period (Fig. 2).

A high *GD* indicates episodes of exceptionally high concentrations of individual PHEs, attributed to various

reasons: intense emissions from local sources, long-range transport of contaminated aerosols (including those from regions experiencing active forest fires), substantial resuspension of soil or road dust particles into the atmosphere, dissolution of solid carbonate particles washed out by acidic rains, etc. For instance, spikes in Sb levels in rainfall on certain days might result from vehicle emissions, the long-range transport of enriched Sb atmospheric aerosols, waste and biomass burning (Gubanova et al. 2021; Ozaki et al. 2021; Serdyukova et al. 2023; Popovicheva et al. 2024). The latter source can also supply P (Meng et al. 2022); and Sr can come from construction sites (Amato et al. 2009). A more detailed analysis of the PHEs' probable sources is given below.

Relationship between PHE concentrations and precipitation properties

Elevated concentrations of Sr during specific episodes are caused by the dissolution of atmospheric particles of construction carbonate dust that is washed out by rain since Sr is often a geochemical companion of Ca and Mg in carbonates (Borsato et al. 2016). The increase in Al, Ce, La,

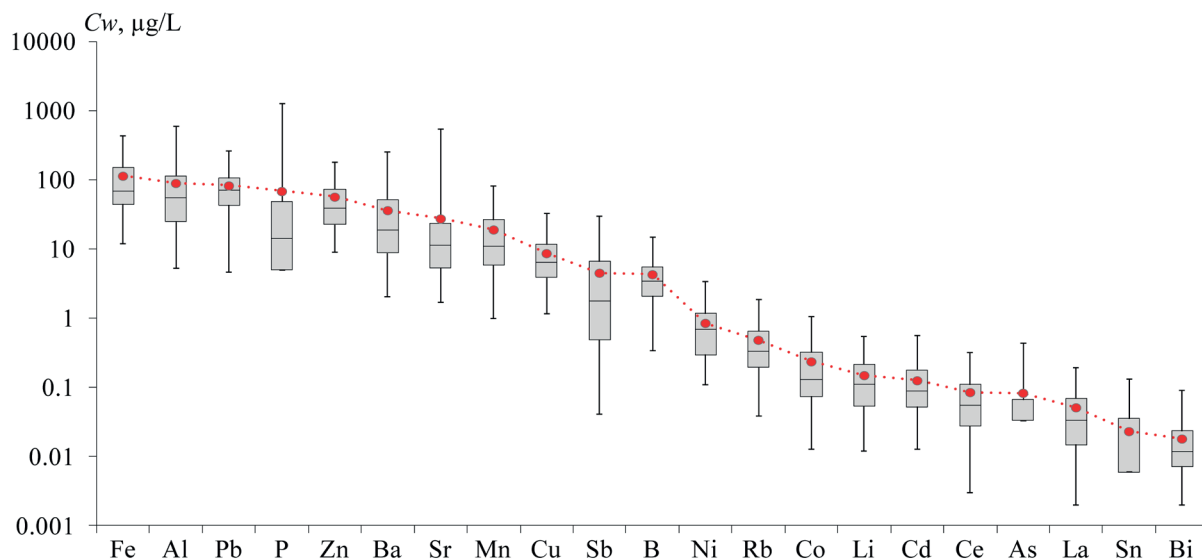


Fig. 1. Volume-weighted concentrations of PHEs in rainwater for the warm season (May–September 2019) on the territory of MO MSU. Elements are ordered by decreasing average concentrations (red dots connected by a red dotted line). "Box" shows 25% and 75% quartiles, line in the "box" shows the median, "whiskers" show minimum and maximum values of PHE concentrations

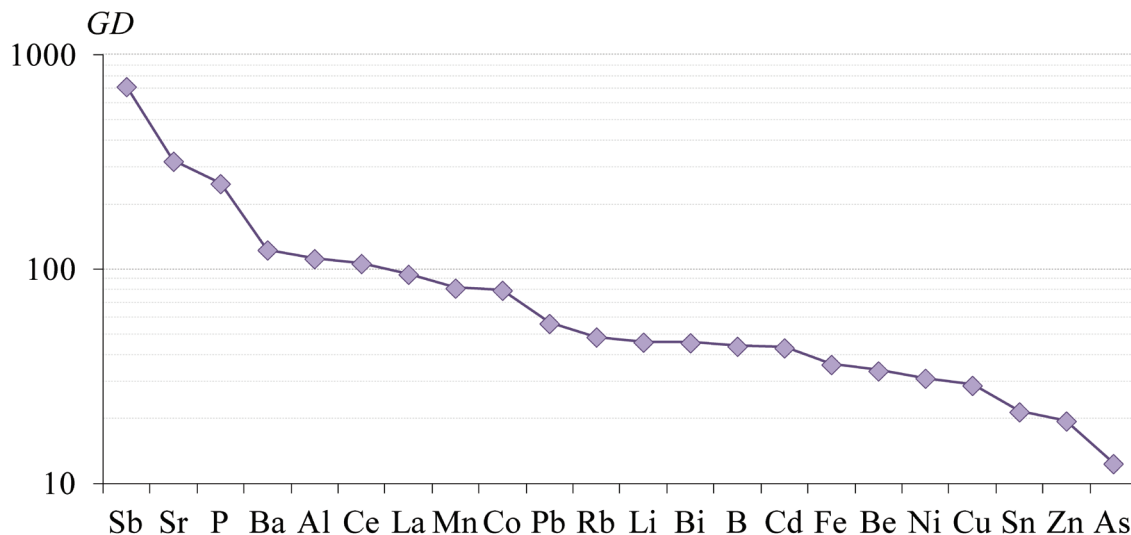


Fig. 2. Geochemical range (*GD*, the ratio of maximum concentrations to minimum) of PHEs in rainwater precipitation from May to September 2019 on the territory of MO MSU

Li, Co, Fe, and other PHE levels may result from soil particle resuspension and their dissolution in acidic rainwater (Amato et al. 2009; Vlasov et al. 2021b,c). This is accompanied by an increase in the content of solid particles in the rain, likely due to prolonged antecedent dry periods, allowing particle accumulation in the atmosphere. This relationship is supported by high Spearman rank correlation coefficients (r_s) between PHE content in solution and solid particles in rain samples (Table 2), ranging from 0.82–0.85 for Co and Mn, 0.74–0.75 for Li, Zn, and Rb, 0.60–0.66 for Be, Ni, Sr, Cd, Bi, La, and Ce, and 0.46–0.59 for other PHEs, except Pb.

Partial dissolution of soil and road dust aerosol components may contribute to an increase in precipitation pH since water extraction from soils and road dust in Moscow has an alkaline reaction (Kosheleva et al. 2018; Kasimov et al. 2019; Vlasov et al. 2022). Under alkaline conditions, anionic elements and some complexing agents can transition from a suspended to a dissolved phase, while cationic PHEs tend to be more soluble in acidic conditions. Thus, significant negative r_s values are observed between the content of specific cationic elements (Li, Al, Fe, Pb) in rainwater and pH, while r_s values for other PHEs are insignificant. Low pH can be both a cause of increased PHE solubility and an indicator of PHE input from industrial emissions and thermal power plants supplying

sulfates, as well as transportation sources that release nitrates, leading to atmospheric precipitation acidification to pH 5 and below. Additionally, chlorides from deicing agents also contribute to the acidification of atmospheric precipitation in Moscow (Eremina et al. 2015; Zappi et al. 2023).

One of the main factors leading to the reduction in PHE levels in rainwater as precipitation increases is linked to dilution (Song and Gao 2009; Park et al. 2015; Ma and Kang 2018), which is sometimes also called the “rain-scour effect” (Zeng et al. 2020). During the warm season in Moscow, dilution effects were observed for all PHEs, most notably for Ni ($r_s = -0.74$), Li (-0.69), Sr (-0.68), Zn (-0.67), Mn (-0.64), Ba (-0.63), Cu (-0.62), Co (-0.61). Specific conductivity, reflecting the presence of readily soluble compounds in rainwater, also decreases with increasing precipitation amounts but rises with PHE concentration in precipitation (Table 2).

These factors influence the varying levels of PHEs in rainwater across different months. Table 3 presents the monthly concentrations of PHEs in rainwater within the MO MSU area during the 2019 warm season.

For comparison of dissolved PHE concentrations across different months, a “growth index” K_s was calculated. The K_s values for May, June, July, August, and September are shown in Fig. 3.

Table 2. Spearman rank correlation coefficients (r_s) between PHE content in rainwater and precipitation amount, pH, specific conductivity (EC), and solid particle content in rainwater (N=56)

PHE	Precipitation amount	pH	EC	Solid particle content
Mn	<i>-0.64</i>	0.26	<i>0.93</i>	<i>0.85</i>
Co	<i>-0.61</i>	0.24	<i>0.91</i>	<i>0.82</i>
Rb	<i>-0.53</i>	0.20	<i>0.88</i>	<i>0.75</i>
Li	<i>-0.69</i>	<i>0.28</i>	<i>0.86</i>	<i>0.74</i>
Zn	<i>-0.67</i>	0.08	<i>0.93</i>	<i>0.74</i>
Sr	<i>-0.68</i>	0.20	<i>0.89</i>	<i>0.66</i>
Cd	-0.24	0.01	<i>0.70</i>	<i>0.66</i>
Be	<i>-0.52</i>	-0.06	<i>0.78</i>	<i>0.65</i>
Bi	<i>-0.41</i>	-0.04	<i>0.78</i>	<i>0.65</i>
Ni	<i>-0.74</i>	0.14	<i>0.90</i>	<i>0.64</i>
Ce	<i>-0.55</i>	-0.13	<i>0.89</i>	<i>0.62</i>
La	<i>-0.57</i>	-0.15	<i>0.91</i>	<i>0.60</i>
As	-0.24	-0.03	<i>0.65</i>	<i>0.59</i>
Cu	<i>-0.62</i>	-0.10	<i>0.88</i>	<i>0.57</i>
B	<i>-0.38</i>	-0.06	<i>0.75</i>	<i>0.53</i>
Al	<i>-0.59</i>	<i>-0.29</i>	<i>0.81</i>	<i>0.50</i>
Ba	<i>-0.63</i>	-0.08	<i>0.80</i>	<i>0.46</i>
Sb	<i>-0.47</i>	-0.20	<i>0.66</i>	<i>0.43</i>
Fe	<i>-0.50</i>	<i>-0.34</i>	<i>0.78</i>	<i>0.41</i>
P	-0.14	-0.12	<i>0.45</i>	<i>0.40</i>
Sn	<i>-0.45</i>	-0.08	<i>0.66</i>	<i>0.39</i>
Pb	-0.19	<i>-0.59</i>	<i>0.39</i>	0.05

Note. Significant r_s levels at $p < 0.05$ are highlighted in bold italics. Elements are ranked by r_s for solid particle content.

Table 3. Monthly volume-weighted concentrations of dissolved PHEs in rainwater on the territory of MO MSU during the 2019 warm season

PHE	Concentration in rainwater, µg/L				
	May	June	July	August	September
Li	0.11 (0.045–0.29)	0.085 (0.034–0.52)	0.064 (0.022–0.29)	0.059 (0.012–0.55)	0.16 (0.080–0.32)
Be	0.007 (0.001*–0.018)	0.005 (0.001*–0.032)	0.004 (0.001*–0.014)	0.003 (0.001*–0.019)	0.007 (0.001*–0.037)
B	4.7 (1.9–8.8)	3.5 (1.4–15)	2.4 (0.66–5.4)	2.8 (0.34–13)	3.9 (1.5–13)
Al	90 (37–590)	34 (5.7–265)	26 (12–149)	41 (5.2–239)	86 (23–348)
P	213 (5.0*–1,259)	72 (14–387)	20 (5.0*–204)	9.2 (5.0*–60)	17 (5.0*–123)
Mn	19 (3.8–57)	9.8 (1.9–77)	7.2 (2.1–36)	7.3 (1.0–82)	15 (7.1–40)
Fe	88 (23–348)	66 (26–382)	55 (20–253)	63 (12–429)	110 (34–403)
Co	0.26 (0.022–1.0)	0.15 (0.054–0.81)	0.089 (0.029–0.46)	0.084 (0.013–0.84)	0.16 (0.069–0.44)
Ni	0.52 (0.11–1.7)	0.45 (0.13–2.6)	0.34 (0.12–1.5)	0.37 (0.11–2.5)	1.1 (0.70–3.4)
Cu	6.4 (1.8–19)	6.6 (2.5–33)	4.6 (2.1–16)	4.0 (1.1–23)	9.2 (2.8–20)
Zn	48 (16–157)	34 (12–178)	27 (11–133)	25 (9.1–164)	46 (19–126)
As	0.14 (0.033*–0.36)	0.048 (0.033*–0.41)	0.033* (0.033*–0.033*)	0.047 (0.033*–0.23)	0.046 (0.033*–0.23)
Rb	0.55 (0.19–1.8)	0.36 (0.18–1.8)	0.24 (0.087–0.80)	0.17 (0.038–1.0)	0.38 (0.15–0.75)
Sr	12 (4.1–36)	7.5 (3.7–42)	7.2 (2.2–72)	7.9 (1.7–71)	48 (5.9–535)
Cd	0.16 (0.036–0.35)	0.11 (0.043–0.56)	0.11 (0.019–0.29)	0.047 (0.013–0.22)	0.12 (0.048–0.45)
Sn	0.019 (0.006*–0.089)	0.010 (0.006*–0.13)	0.008 (0.006*–0.056)	0.011 (0.006*–0.043)	0.023 (0.006*–0.081)
Sb	5.5 (2.3–18)	0.20 (0.041–1.6)	0.79 (0.14–13)	3.4 (0.53–29)	2.6 (0.88–11)
Ba	28 (13–92)	6.5 (2.0–42)	10 (5.1–69)	19 (3.2–130)	51 (11–252)
La	0.047 (0.012–0.14)	0.034 (0.006–0.19)	0.018 (0.005–0.091)	0.023 (0.002–0.16)	0.043 (0.010–0.11)
Ce	0.079 (0.019–0.25)	0.057 (0.009–0.32)	0.033 (0.012–0.14)	0.039 (0.003–0.27)	0.065 (0.019–0.17)
Pb	84 (22–258)	99 (53–161)	56 (24–140)	41 (9.0–214)	66 (4.6–225)
Bi	0.019 (0.006–0.091)	0.023 (0.006–0.064)	0.008 (0.002*–0.033)	0.006 (0.002*–0.025)	0.013 (0.007–0.027)

Note: Average monthly concentrations of PHEs are provided, with minimum and maximum concentrations in parentheses.

*Concentration as half the limit of detection LOD

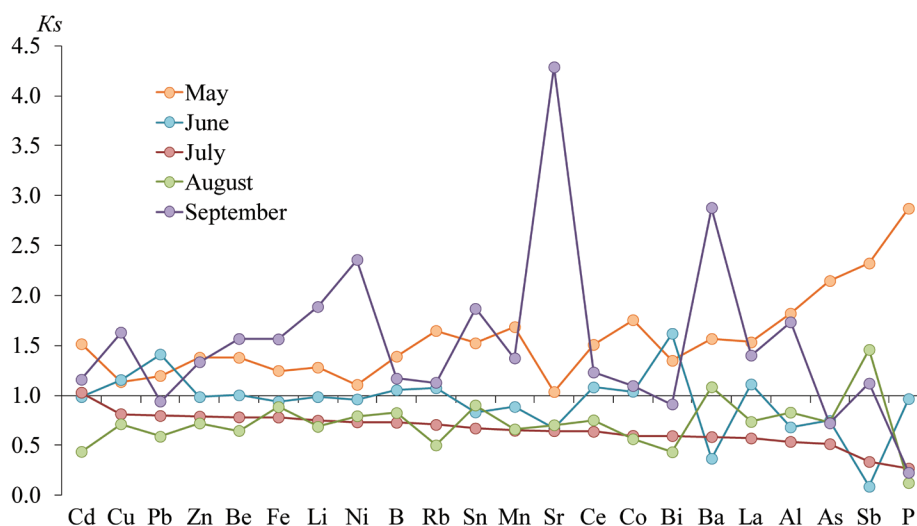


Fig. 3. The levels of growth index (K_s) for PHEs in precipitation on the territory of MO MSU. K_s shows the ratio between the concentration of PHE in individual months of 2019 relative to the average concentration of the same PHE over the entire study period (May–September 2019)

In May, concentrations of all PHEs, and in September, concentrations of all PHEs, except Pb, Bi, As, and P, were higher than the average for the entire warm season (Fig. 3). Significant pollution by Sb, Cd, Cu, Pb, Bi, Sn, Zn, and B in May can be attributed to increased transportation activity due to the beginning of the active suburban travel season. Additionally, the burning of large quantities of plant residues in suburban areas and wood coal in forest parks during the May holidays contributed to the release of As, Rb, P, Sb, Sn, and Cd into the atmosphere. Active transport of plant pollen containing P, Mn, Cu, and Zn also played a role. Immature vegetation cover and large open soil areas also impacted the emission of enriched particles (especially Al, Ce, La, Fe, Mn, Rb, Sr, and Ba), increasing PHE levels in precipitation.

During the summer, a reduction in the transport load due to the holiday season and the end of the school year, along with a decrease in the surface area of soils with sparse vegetation cover, caused many of these factors to diminish. This led to lower PHE concentrations in summer rains compared to the warm-season average. July recorded the lowest pollutant concentrations due to relatively high rainfall and prevailing cyclonic circulation with effective dispersion of contaminants (Table 1).

In September, high PHE concentrations in rain were associated with significantly lower precipitation (21.3 mm), which was 65% below the monthly norm and also notably less than in other months (Table 1). This resulted in reduced dilution and, consequently, higher PHE concentrations. Moreover, in September, many residents returned from vacations, transportation loads increased, work on harvesting and preparing for the cold season (including burning of plant residues) was carried out in suburban territories, non-vegetated soil areas increased, and the heating season began at the end of the month, leading to increased emissions of PHEs into the atmosphere and consequently higher concentrations of chemical elements in rainwater. The highest K_s in September was found for Sr, possibly due to intensified construction and road works near the MO MSU area, which released a large amount of carbonate dust enriched with this metal. The P content in September rains was lower than the warm-season average, as well as the levels in May, June, and July, possibly due to the reduced role of plant pollen in the transport of this element in autumn compared to spring (the highest K_s for P was noted in May).

Regions of air advection and their influence on the content of PHEs in rains

Figure 4 illustrates the variations in total normalized concentrations (NM) from May to September 2019. Several episodes exhibited notably high concentrations of PHEs in rainwater: the May holiday period (May 2–8), May 13, June 8 and 22, July 14 and 31, August 2 and 15, September 5 and 18. We previously found that the May holiday period was characterized by active traffic loads and resuspension of soil and road dust particles, leading to a sharp increase in the concentrations of soluble and particulate-bound insoluble PHEs in atmospheric precipitation (Chubarova et al. 2020; Vlasov et al. 2021b, 2023a). Additionally, biomass burning and forest fires contributed substantially to atmospheric aerosol pollution, as indicated by elevated black carbon concentrations (Popovicheva et al. 2020).

Between May 2 and 8, as well as on May 13, Moscow experienced prevailing air advection from Southern Europe and the southern regions of European Russia, where agricultural activities causing soil wind erosion and forest and agricultural fires were intensified (Fig. 5). Emissions from thermal power plants could have also exerted an additional influence on precipitation pollution during this period since the obtained backward trajectories pass over areas with large coal-fired power plants in Southern Europe and European Russia (Global Coal Plant Tracker 2024). In other episodes with high normalized PHE concentrations (June 8 and 22, July 14, and September 5), regional sources significantly influenced air and precipitation pollution (Fig. 5).

At the end of July and the beginning of August, air advection from the north of Western Siberia prevailed, resulting in PHE contamination in precipitation due to forest fires and emissions from oil and gas extraction facilities (Fig. 6), as confirmed by NASA data on fire outbreaks along the path of air masses (FIRMS 2024). During rainfall events on August 15 and September 18, air advection from the northern parts of Europe predominated (Fig. 6).

Episodes of precipitation with low normalized PHE concentrations in rainwater are notably distinct. These include episodes on May 16, June 29, and September 22, when air advection from the North Atlantic prevailed, on July 12 from the Arctic, and on July 20 and August 10 from the Arctic and the northern regions of Northern Europe (Fig. 6).

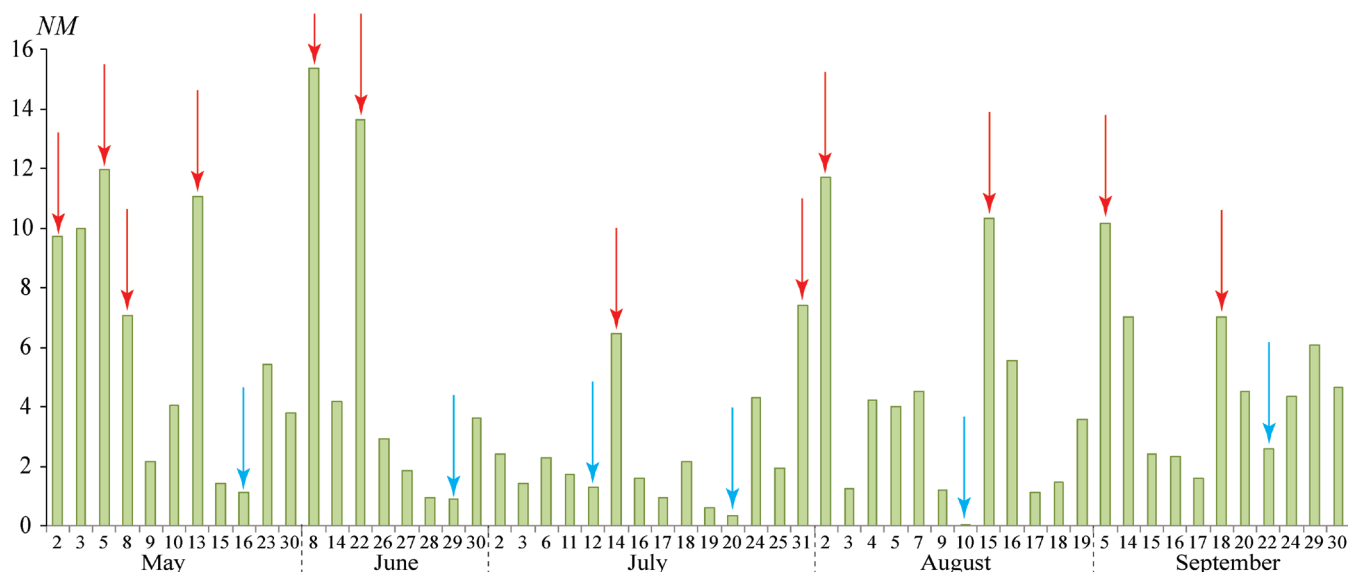


Fig. 4. Normalized concentrations of PHEs (NM) in atmospheric precipitation on the territory of MO MSU during the warm season of 2019. Red arrows indicate episodes with a significant increase in normalized concentrations relative to other days; blue arrows indicate a significant decrease. For some of these episodes, calculations of backward trajectories are presented in Fig. 5 and Fig. 6

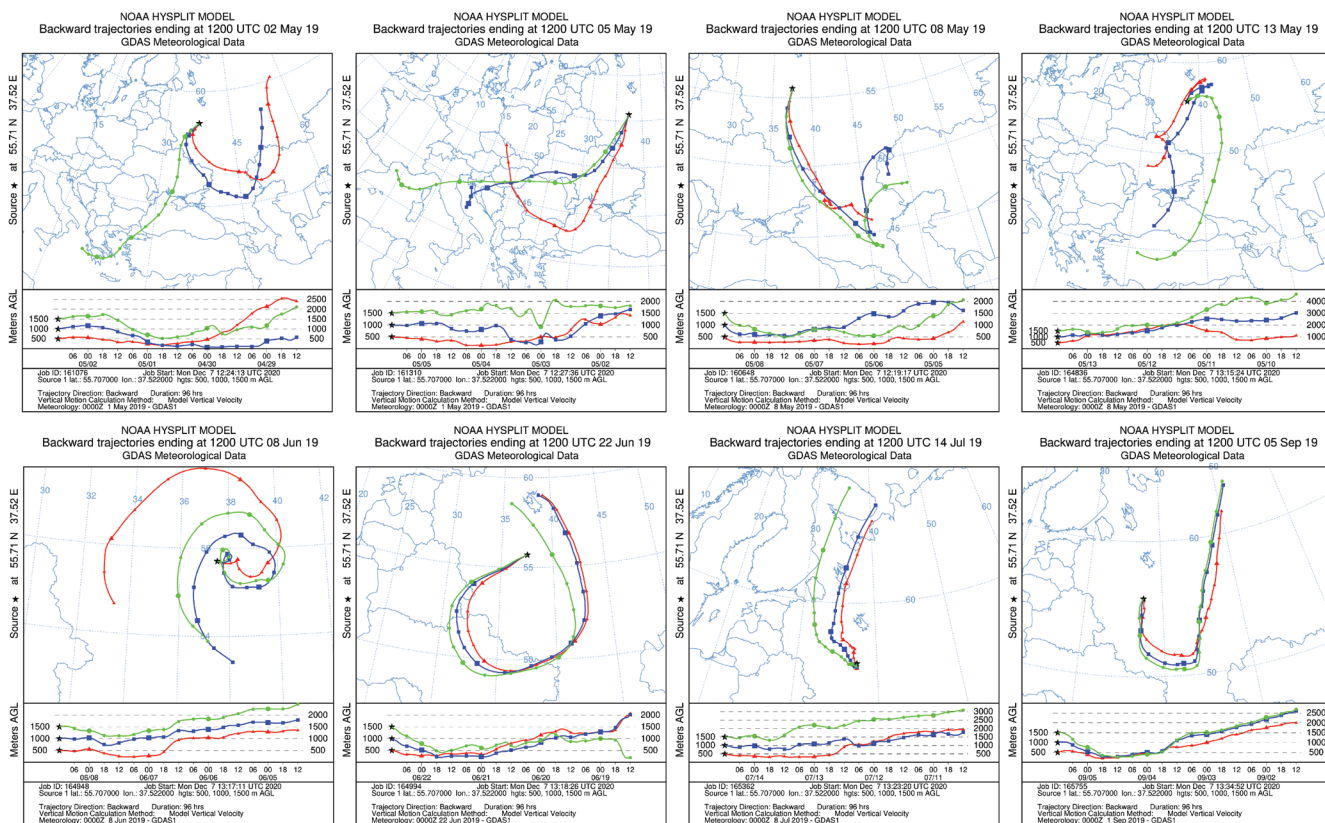


Fig. 5. Backward trajectories (NOAA HYSPLIT) with an endpoint at the MO MSU for dates with a high content of PHEs in precipitation: upper graphs show advection from Southern Europe and southern Russia (May 2, 5, 8, and 13); lower graphs show the impact of regional sources of pollution (June 8 and 19, July 14, and September 19)

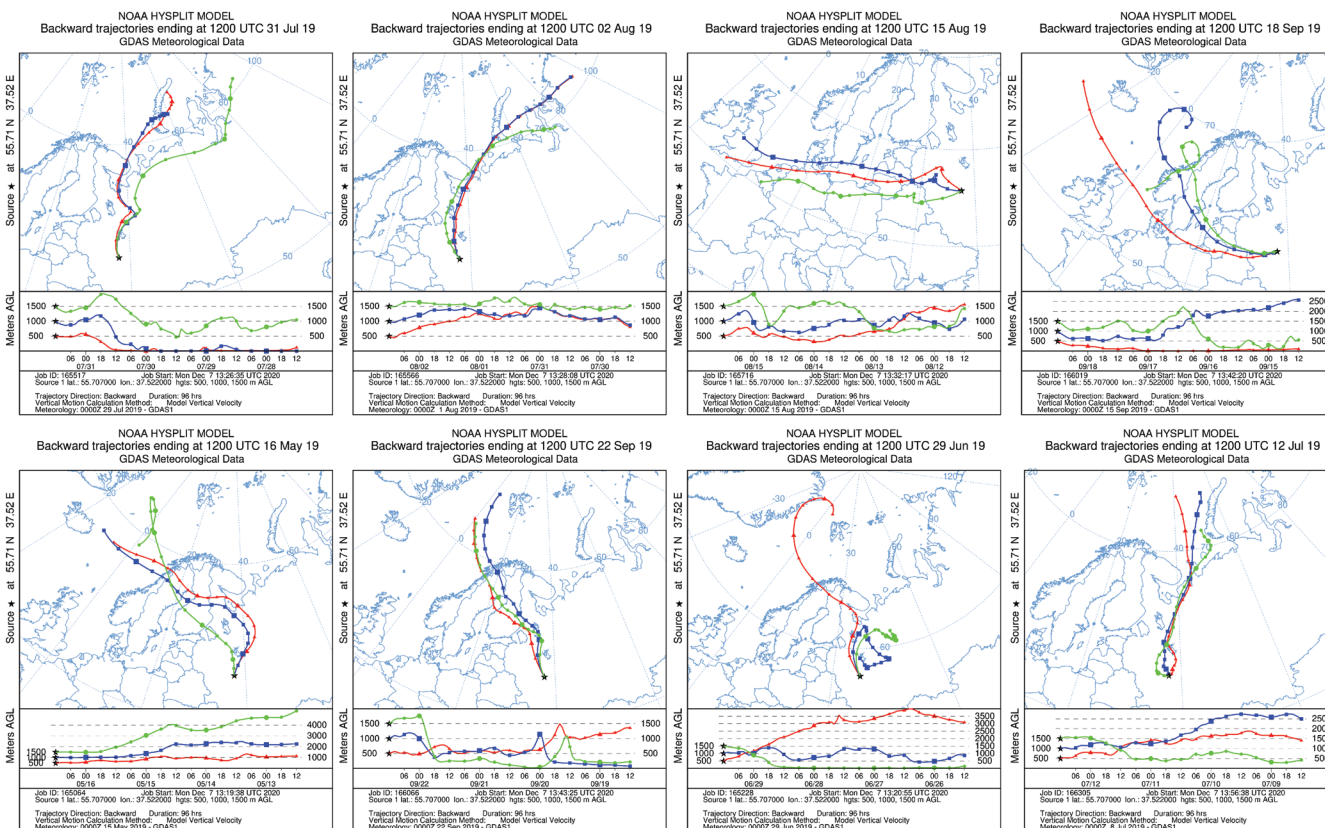


Fig. 6. Backward trajectories (NOAA HYSPLIT) with an endpoint at the MO MSU for dates with the high and low contents of PHEs in precipitation. The upper graphs are made for dates with a high content of PHEs in precipitation during advection from the north of Western Siberia and the Urals (July 31 and August 2), Northern and Western Europe (August 15 and September 18); lower graphs are made for dates with low PHEs content in precipitation during advection from the North Atlantic (May 16, June 29, and September 22) and from the Arctic (July 12)

Sources of potentially hazardous elements

Figure 7 presents the average, median, minimum, and maximum EF values in Moscow rains during the warm season. The highest levels of enrichment, indicating clear anthropogenic sources, are observed for Sb (average $EF = 10,317$), Pb (8,348), Cd (2,233), Zn (1,113), Cu (420), B (365), and Bi (167). P (180) and Sr (131) also belong to this group; however, the influence of anthropogenic sources for these two elements is only evident during specific precipitation episodes, primarily in May and June for P and in September for Sr.

The most probable and active sources of Sb, Cd, Zn, Cu, B, and Bi are non-exhaust vehicle emissions, such as wear and tear of clutch components, brake systems, tires, and road surfaces, along with the resuspension of road dust and soil particles. For instance, brake pads and linings contain Cu, Sb sulfides, Zn borates, and other compounds (European Borates Association 2011, Hulskotte et al. 2014; Grigoratos and Martini 2015; Alves et al. 2018; Budai and Clement 2018; Ramírez et al. 2019). Similarly, tires contain significant amounts of Zn and Cd, making tire abrasion a source of PHEs in the atmosphere (Harrison et al. 2012; Pant and Harrison 2013). In Moscow, the resuspension of road dust can significantly contribute to air and precipitation pollution. It is known that road dust, especially its fine fractions with diameters less than $10\ \mu\text{m}$ (PM_{10}) and less than $1\ \mu\text{m}$ (PM_1), is highly enriched with Sb, Zn, Pb, Cd, Bi, Sn, and W (Fedotov et al. 2014; Ermolin et al. 2018; Kasimov et al. 2020, 2024; Ladonin and Mikhaylova 2020; Vlasov et al. 2021c, 2023b; Ivaneev et al. 2023; Kolesnikova et al. 2023; Vetrova et al. 2023).

PHEs can additionally originate from industrial emissions in the city, particularly from metal processing and engineering plants, non-ferrous metal treatment, metallic parts manufacturing, etc. (Demetriades and Birke 2015; Zheng et al. 2018; Serdyukova et al. 2023). Additionally, they can be emitted during the resuspension of contaminated particles from urban soils (Gunawardana et al. 2012; Harrison et al. 2012; Padoan et al. 2016; Morera-Gómez et al. 2020; Konstantinova et al. 2022; Moskovchenko et al. 2022). In Moscow, the top horizons of urban soils are contaminated with Pb, Cu, Cd, Zn, Bi, Sn, W, Cr, Mo, and other PHEs (Kosheleva et al. 2015, 2018; Ermakov et al. 2017; Romzaykina et al. 2021; Vlasov et al. 2022). Soil particles can serve as significant sources of Sr and P, while Sr primarily

originates from carbonate construction dust emissions and dust generated during building demolition (Amato et al. 2009), and P comes from bioaerosols, biomass burning, forest fires, and asphalt wear (Feddes et al. 1992; Yang et al. 2011; von Gunten et al. 2020; Wada et al. 2020; Meng et al. 2022). Fires and controlled biomass and waste burning can also be sources of other PHEs with high EF s, such as Sb, Pb, Cd, Bi, Zn, and Cu (Kumar et al. 2015; Jain et al. 2018; Bencharif-Madani et al. 2019).

The factors mentioned above play a lesser role in enriching atmospheric precipitation with the second group of PHEs, characterized by moderate EF levels ranging from 10 to 100: Ba ($EF = 69$), Mn (31), As (24), Ni (24), Co (18), and Sn (15). These PHEs are predominantly emitted during biomass and waste burning and the resuspension of soil particles (Christian et al. 2010; Niyobuhungiro and Blotnitz 2013; Konstantinova et al. 2024). The third group mainly comprises PHEs originating from natural (terrigenous) sources such as soils, rocks, and the transport of background aerosols. In Moscow's precipitation, this group includes Li ($EF = 9$), Rb (8), Be (4), Fe (3), rare earths La (1.8) and Ce (1.5), as well as Al. In small quantities, Rb can be emitted during the combustion of plant residues and coal (Grivas et al. 2018), while Fe originates from road dust particles, emissions from metal processing facilities, and mechanical abrasion of metallic vehicle parts (Grigoratos and Martini 2015). Thus, the contribution of the second and third groups of PHEs to atmospheric precipitation is sporadically linked to anthropogenic influence, with the highest contribution often coming from mixed natural-anthropogenic sources (resuspension of contaminated soil and road dust) and natural sources (long-range transport of background aerosols and rock particles).

Multivariate regression analysis of factors contributing to the accumulation of PHEs in atmospheric precipitation

The collected data were analyzed through multivariate regression to quantitatively assess the role of factors influencing the accumulation of PHEs in rainwater. The regression tree method was used, with dendrograms constructed to illustrate the relationship between the concentrations of individual elements and three groups of factors: (1) meteorological conditions, including the amount of atmospheric precipitation and the duration of the antecedent dry period; (2) below-cloud interactions,

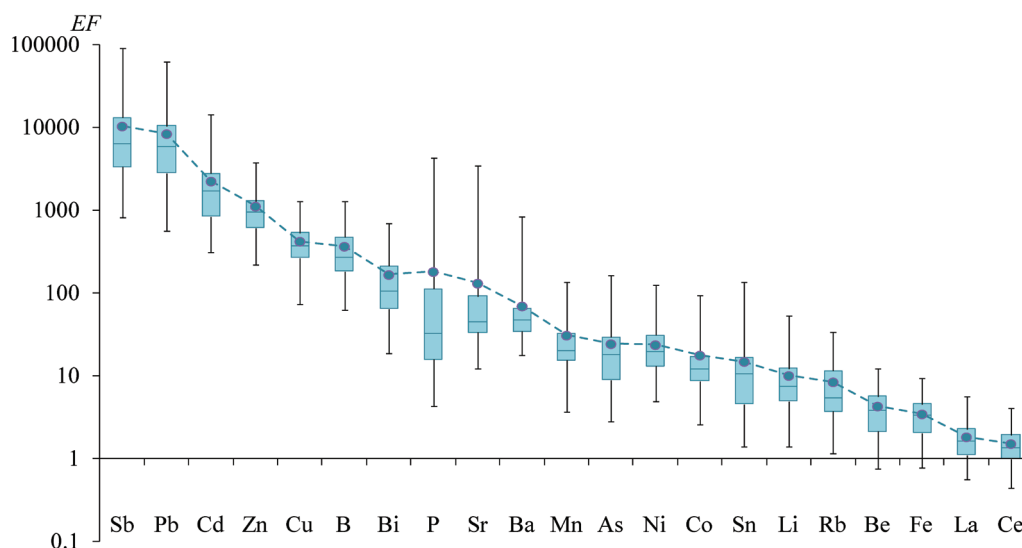


Fig. 7. Enrichment factors (EF) for PHEs in atmospheric precipitation on the territory of MO MSU in May–September 2019. PHEs are ordered by decreasing mean EF values (dots connected by a dotted line). “Box” shows 25% and 75% quartiles, the line in the “box” shows the median, “whiskers” show minimum and maximum EF values

characterized by the pH of precipitation and the content of solid particles in rainwater; and (3) long-range transport, which determines the influx of PHEs from various regions identified through backward trajectory analysis.

The calculations revealed that for most PHEs, namely Li, Zn, La, Ce, Mn, Co, Rb, Sb, As, Bi, Cd, Sn, and P, solid particles are the primary factor intensifying their concentration in atmospheric precipitation. The partial dissolution of this material contributes to rainwater pollution (Table 4). In second place in importance, this factor was identified for Ni, Be, and Fe, while in third place, it was found for Li, Cu, Zn, La, Ce, B, Al, Bi, and Cd. For Al and Pb, precipitation acidity emerged as the primary accumulation factor, likely associated with the partial dissolution of solid particles. This is because the solubility of these elements increases significantly with a considerable reduction in the solution's pH, as previously demonstrated in spring precipitation in Moscow (Vlasov et al. 2021b). The pH level is the second most significant accumulation factor for Sb and P, and it is the third for Rb, Be, Fe, Pb, Bi, and Cd.

The length of the antecedent dry period preceding rainfall, an increase of which contributes to the accumulation of pollutants in the atmosphere (which are subsequently washed away by rain), notably impacts the accumulation of Be and B in precipitation. This factor ranks second in importance for Cu, Pb, As, Bi, Sr, and Ba, and third for La, Mn, Pb, and Sn. The primary factor affecting the content of soluble Ni, Fe, Cu, Sr, and Ba in rainwater is the amount of precipitation. An increase in precipitation tends to decrease the level of contamination by these metals due to dilution. This factor ranks second in importance for Li, Zn, Ce, Mn, Co, Rb, Al, Pb, and Sn, and third for Ni, Cu, Be, B, Sb, and Fe.

Long-range transport from other regions significantly contributes to the accumulation of most PHEs, ranking additionally as the second most significant factor for Cu, Mn, Rb, B, Fe, and Cd. Advection from Northern and Northwestern Europe leads to a noticeable increase in La, Ce, Rb, B, Sb, Al, Pb, As, Bi, Cd, and Sn concentrations. Significant rises in the levels of Li, Cu, Zn, La, Ce, Mn, Co, Rb, Be, B, Sb, Al, Fe, As, Bi, Cd, Sn, P, and Ba are observed during advection from the northern European Russia and Western Siberia. Conversely, advection from the southwest of European Russia, Southern Europe, and the Mediterranean typically results in increases in Li, Cu, Be, B, Sb, Al, Fe, Bi, Cd, Sn, and Ba content. Furthermore, regional sources in the central part of European Russia supply Li, Cu, Ce, Mn, Co, Sb, Al, Fe, Sn, and P.

An analysis of dendrograms for Sb, Pb, Cd, and Zn, characterized by the highest EFs, is of particular interest. It is essential to identify combinations of influencing factors that lead to their minimum and maximum concentrations (Fig. 8).

The predominant factor influencing the concentration of Sb in atmospheric precipitation in Moscow is the presence of solid particles in rainwater. When their content exceeds 53 mg/L, the Sb concentration increases by 3.3 times, presumably due to the transition of Sb from suspended matter to solution (Fig. 8a). Conversely, when the suspended matter content is < 53 mg/L, Sb concentrations increase by 3.6 times in acidic precipitation with a pH < 4.5 compared to precipitation with a pH > 4.5. In the latter scenario, the reduction in Sb concentration due to dilution is influenced by the amount of precipitation, particularly at levels above 3.4 mm, resulting in a fourfold decrease in the metalloid content. Although atmospheric

Table 4. Factors of PHEs accumulation in atmospheric precipitation on the territory of MO MSU during the warm season of 2019

Factors		Li	Ni	Cu	Zn	La	Ce	Mn	Co	Rb	Be	B	Sb	Al	Fe	Pb	As	Bi	Cd	Sn	P	Sr	Ba
Below-cloud interactions	pH	N/A	N/A	N/A	4-	N/A	N/A	N/A	N/A	3-	3-	4-	2-	1-	3-	1-, 3-	N/A	3-	3-	N/A	2-	N/A	N/A
	Solid particle content	1+, 3+	2+, 4+	3+	1+, 3+, 4+	1+, 3+	1+, 3+	1+	1+	1+	2+, 4+	3+	1+, 5+	3+	2+, 4+	4+	1+	1+, 3+	1+, 3+	1+	1+	N/A	N/A
Meteorological conditions	Amount of precipitation	2-	1-, 3-	1-, 3-	2-	2-, 5-	2-	2-	2-	2-	3-	3-	3-	2-	1-, 3-	2-	N/A	5-	N/A	2-	N/A	1-	1-
	Antecedent dry period	N/A	N/A	2+	N/A	3+	N/A	3+	N/A	4+	1+	1+	N/A	N/A	N/A	2+, 3+	2+	2+	N/A	3+	N/A	2+	2+
Long-range transport	A	4+	N/A	2-	3+	4+	3+, 4-	2+	3+	2-	4+	2-	4-	3-	2-, 4+	3-	3-	4-	2-, 4-	4-, 4+	3+	N/A	3-
	B	4+	N/A	2+	3+	4+	3+, 4-	2+	3+	2+	4+	2+	4+, 4-	3+	2+	N/A	3+	4+	2+	4+	3-	N/A	3+
	C	4-	N/A	2-	3-	4-	3-, 4+	2+	3-	2+	4-	2-	4-, 4+	3-	2-, 4-	3-	3-	4+	2-, 4+	4-	3+	N/A	3+
	D	4-	N/A	2-	3-	4+	3-, 4+	2-	3-	2+	4-	2+	4+, 4-	3+	2-, 4-	3+	3+	4+	2+	4+, 4-	3-	N/A	3-
	E	4+	N/A	2+	3-	4-	3-	2-	N/A	2-	4+	2+	4-, 4+	3+	2-, 4+	3-	3-	4+	2+	4+, 4-	3-	N/A	3+
	F	4+	N/A	2-	3-	4-	3-, 4+	2+	3-	2-	4-	2+	4-, 4+	3-	2-, 4-	3+	3-	4-	2-, 4+	4+	3-	N/A	3-
	G	4+	N/A	2+	3-	4-	3+, 4-	2+	3+	2-	N/A	2-	4+	3+	2+	3-	3-	4-	2-, 4-	4-, 4+	3+	N/A	3-

Note: Ranks from 1 to 5 indicate a decrease in the significance of the factor: "+" shows a situation where an increase in the indicator contributes to an increase in the concentration of PHE, "-" shows a situation where an increase in the indicator contributes to a decrease in the concentration of PHE. Regions of advection (long-range transport): A, northern European Russia, Arctic; B, northern European Russia, Arctic, Western Siberia; C, North Atlantic and Scandinavia; D, Northern and Northwestern Europe; E, southwest of European Russia, Ukraine, Southern Europe, Mediterranean; F, the southern part of European Russia and northwestern Kazakhstan; G, the center of European Russia (regional sources). N/A, not available.

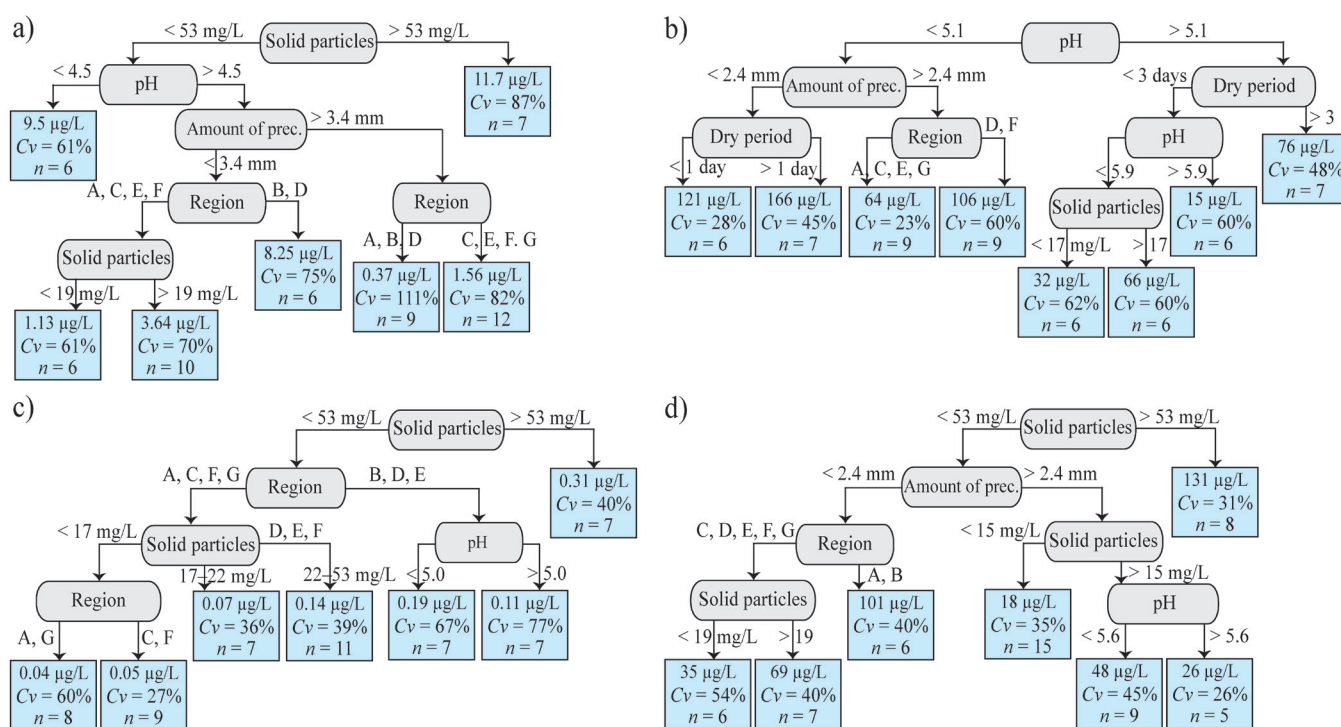


Fig. 8. Factors of accumulation of Sb (a), Pb (b), Cd (c), Zn (d) in atmospheric precipitation in Moscow. Regions of advection (long-range transport): A, northern European Russia, Arctic; B, northern European Russia, Arctic, Western Siberia; C, North Atlantic and Scandinavia; D, Northern and Northwestern Europe; E, southwest of European Russia, Ukraine, Southern Europe, Mediterranean; F, southern part of European Russia and northwestern Kazakhstan; G, center of European Russia (regional sources)

advectations have minimal impact, elevated Sb levels are attributed to sources in northern European Russia and Western Siberia, as well as during advectations from Northern and Northwestern Europe.

The primary accumulation factor for Pb is pH. In acidic rainwater with a pH < 5.1, Pb concentrations tend to double (Fig. 8b), especially with a precipitation amount of less than 2.4 mm. Moreover, rainwater pollution with Pb intensifies with more extended antecedent dry periods. A rise in Pb concentrations in precipitation occurs when air masses originate from regions D and F, namely, during advection from Northern and Northwestern Europe, from the southern part of European Russia, and from the northwest part of Kazakhstan. The alkalization of precipitation with a pH > 5.9 reduces the solubility of Pb, leading to its minimal concentrations.

The main determinant for Cd, similar to Sb, is the content of solid particles in precipitation, with a similar threshold of 53 mg/L delineating sample divisions, above which Cd concentrations in rainwater triple (Fig. 8c). When suspended matter concentrations are below 53 mg/L, the region of advection significantly influences Cd content in rainwater: Cd levels increase during advectations from the northern regions of European Russia and Western Siberia, as well as from Northern and Northwestern Europe, the southwest of European Russia, Southern Europe, and the Mediterranean, especially when precipitation pH is below 5.0.

It is noteworthy that Zn follows a similar pattern, with the solid particle content threshold above which metal concentrations increase by 2.9 times also being 53 mg/L (Fig. 8d). When suspended matter concentrations fall below 53 mg/L, Zn content in rainfall is influenced by the amount of precipitation: upon exceeding an amount of 2.4 mm, metal content decreases by 2.4 times due to dilution, and an increase in rainfall acidity is accompanied by a slight rise in Zn concentrations. With amounts less than 2.4 mm, precipitation pollution with Zn intensifies, driven by regional sources situated in the central part of European

Russia as well as during advectations from the northern regions of European Russia and Western Siberia.

CONCLUSIONS

The research has confirmed a significant role of atmospheric precipitation in washing out PHEs from the atmosphere. The concentrations of all PHEs in May, and the content of all PHEs, except Pb, Bi, As, and P, in September, exceeded the warm season's average. Significant contamination of precipitation in May is associated with heavy traffic activity during the vacation season, extensive burning of plant residues and wood during the May holidays, and pollen dispersion. During the summer months, with the reduction of significant forest and agricultural fires, the decrease in vehicular traffic, and the development of grass and deciduous cover, the concentrations of most PHEs decrease. This trend is particularly evident in July, when typical amounts of atmospheric precipitation occur due to active convection in cyclonic conditions, aiding in the dispersion of pollutants. In September, against the backdrop of a small amount of precipitation, there is an increase in PHE concentrations due to increased transportation activity, intense biomass burning during agricultural activities, and the expansion of unvegetated soil areas.

For the first time, data obtained for Moscow on the distribution of PHEs in atmospheric precipitation during the warm season showed significant enrichment of rainwater with Sb ($EF > 10,000$), Pb ($> 8,000$), Cd, Zn (1,000–2,000), Cu, B, Bi, P, and Sr (100–500). The main sources of PHEs are non-exhaust vehicle emissions, resuspension of contaminated soil particles, emissions from industrial facilities, transport of construction dust, biomass and waste burning, and forest fires. Additionally, precipitation shows moderate enrichment with Ba, Mn, Ni, Co, and Sn (EF 15–69), with their input from the mentioned sources occurring episodically. The content of PHEs increases with reduced precipitation amounts and increased levels of solid particles and pH in rainwater.

Multivariate regression analysis identified the leading factors affecting PHE concentrations in Moscow's precipitation. For most elements, solid particles serve as a significant source of PHEs, with their accumulation in the atmosphere increasing with the duration of dry periods and their partial dissolution being particularly pronounced in acidic rainfall. During the warm period of 2019, long-range transport was also a significant factor: episodes with very high concentrations of PHEs in rainwater were identified, during which air advection from Southern Europe and southern regions of European Russia predominated, or the contribution of regional pollution sources dominated, or a significant contribution was made by advection from the north of Western Siberia, where forest fires were observed.

When air advection occurred from the North Atlantic, the Arctic, and the northern part of Northern Europe, PHE concentrations in precipitation generally decreased, but some elements (Rb, Sb, Pb, As, Bi, Cd, P, Ba) increased their content.

A limitation of the obtained results is the analysis of only the dissolved phase of PHEs in rainfall, whereas the insoluble phase can be an essential form for some PHEs in precipitation. Therefore, further research is needed to include the analysis of the insoluble phase of PHEs. Additionally, to assess more accurately the influence of various sources, it is necessary to study the seasonal and interannual variability of atmospheric pollution. ■

REFERENCES

- Adhikari S., Zeng C., Zhang F., Paudel Adhikari N., Gao J., Ahmed N., Quaiyum Bhuiyan M.A., Ahsan M.A., and Rahaman Khan M.H. (2023). Atmospheric wet deposition of trace elements in Bangladesh: A new insight into spatiotemporal variability and source apportionment. *Environmental Research*, 217, 114729, DOI: 10.1016/j.envres.2022.114729.
- Alves C.A., Evtugina M., Vicente A.M.P., Vicente E.D., Nunes T.V., Silva P.M.A., Duarte M.A.C., Pio C.A., Amato F., and Querol X. (2018). Chemical profiling of PM10 from urban road dust. *Science of The Total Environment*, 634, 41–51, DOI: 10.1016/j.scitotenv.2018.03.338.
- Amato F., Pandolfi M., Viana M., Querol X., Alastuey A., and Moreno T. (2009). Spatial and chemical patterns of PM10 in road dust deposited in urban environment. *Atmospheric Environment*, 43 (9), 1650–1659, DOI: 10.1016/j.atmosenv.2008.12.009.
- Bayramoğlu Karşı M.B., Yenisoğ-Karakaş S., and Karakaş D. (2018). Investigation of washout and rainout processes in sequential rain samples. *Atmospheric Environment*, 190, 53–64, DOI: 10.1016/j.atmosenv.2018.07.018.
- Bencharif-Madani F., Ali-Khodja H., Kemmouche A., Terrouche A., Lokorai K., Naidja L., and Bouziane M. (2019). Mass concentrations, seasonal variations, chemical compositions and element sources of PM10 at an urban site in Constantine, northeast Algeria. *Journal of Geochemical Exploration*, 206, 106356, DOI: 10.1016/j.gexplo.2019.106356.
- Bezrukova N.A. and Chernokulsky A.V. (2023). Russian studies on clouds and precipitation in 2019–2022. *Izvestiya, Atmospheric and Oceanic Physics*, 59 (S3), S294–S325, DOI: 10.1134/S0001433823150033.
- Borsato A., Johnston V.E., Frisia S., Miorandi R., and Corradini F. (2016). Temperature and altitudinal influence on karst dripwater chemistry: Implications for regional-scale palaeoclimate reconstructions from speleothems. *Geochimica et Cosmochimica Acta*, 177, 275–297, DOI: 10.1016/j.gca.2015.11.043.
- Budai P. and Clement A. (2018). Spatial distribution patterns of four traffic-emitted heavy metals in urban road dust and the resuspension of brake-emitted particles: Findings of a field study. *Transportation Research Part D: Transport and Environment*, 62, 179–185, DOI: 10.1016/j.trd.2018.02.014.
- Cable E. and Deng Y. (2018). Trace elements in atmospheric wet precipitation in the Detroit metropolitan area: Levels and possible sources. *Chemosphere*, 210, 1091–1098, DOI: 10.1016/j.chemosphere.2018.07.103.
- Chon K., Kim Y., Bae D.H., and Cho J. (2015). Confirming anthropogenic influences on the major organic and inorganic constituents of rainwater in an urban area. *Drinking Water Engineering and Science*, 8 (2), 35–48, DOI: 10.5194/dwes-8-35-2015.
- Christian T.J., Yokelson R.J., Cardenas B., Molina L.T., and Engling G. (2010). Trace gas and particle emissions from domestic and industrial biofuel use and garbage burning in central Mexico. *Atmospheric Chemistry and Physics*, 10, 565–584, DOI: 10.5194/acp-10-565-2010.
- Chubarova N.E., Nezval' E.I., Belikov I.B., Gorbarenko E.V., Eremina I.D., Zhdanova E.Yu., Korneva I.A., Konstantinov P.I., Lokoshchenko M.A., Skorokhod A.I., and Shilovtseva O.A. (2014). Climatic and environmental characteristics of Moscow megalopolis according to the data of the Moscow State University Meteorological Observatory over 60 years. *Russian Meteorology and Hydrology*, 39 (9), 602–613, DOI: 10.3103/S1068373914090052.
- Chubarova N., Zhdanova Y., Androsova Y., Kirsanov A., Shatunova M., Khlestova Y., Volpert Y., Poliukhov A., Eremina I., Vlasov D., Popovicheva O., Ivanov A., Gorbarenko Y., Nezval Y., Blinov D., and Rivin G. (2020). The aerosol urban pollution and its effects on weather, regional climate and geochemical processes. Moscow, Russia: LLC MAKSS Press.
- Chubarova N., Androsova E., Kirsanov A., Varentsov M., and Rivin G. (2024). Urban aerosol, its radiative and temperature response in comparison with urban canopy effects in megacity based on COSMO-ART modeling. *Urban Climate*, 53, 101762, DOI: 10.1016/j.uclim.2023.101762.
- Chudaeva V.A., Chudaev O.V., and Yurchenko S.G. (2008). Chemical composition of precipitation in the southern part of the Russian Far East. *Water Resources*, 35 (1), 58–70, DOI: 10.1134/S0097807808010077.
- Demetriades A. and Birke M. (2015). Urban topsoil geochemical mapping manual: URGE II; 2015 International Year of Soils. Brussels: EuroGeoSurveys.
- Eremina I.D., Aloyan A.E., Arutyunyan V.O., Larin I.K., Chubarova N.E., and Yermakov A.N. (2015). Acidity and mineral composition of precipitation in Moscow: Influence of deicing salts. *Izvestiya, Atmospheric and Oceanic Physics*, 51 (6), 624–632, DOI: 10.1134/S0001433815050047.
- Ermakov V., Perelomov L., Khushvakhtova S., Tyutikov S., Danilova V., and Safonov V. (2017). Biogeochemical assessment of the urban area in Moscow. *Environmental Monitoring and Assessment*, 189 (12), 641, DOI: 10.1007/s10661-017-6363-y.
- Ermolin M.S., Fedotov P.S., Ivanev A.I., Karandashev V.K., Fedyunina N.N., and Burmistrov A.A. (2018). A contribution of nanoscale particles of road-deposited sediments to the pollution of urban runoff by heavy metals. *Chemosphere*, 210, 65–75, DOI: 10.1016/j.chemosphere.2018.06.150.
- European Borates Association (2011). Borates. [online] Available at: https://www.ima-europe.eu/sites/ima-europe.eu/files/minerals/Borate_An-WEB-2011.pdf [Accessed 28 July 2020].
- Feddes J.J.R., Cook H., and Zuidhof M.J. (1992). Characterization of airborne dust particles in turkey housing. *Canadian Agricultural Engineering*, 34, 273–280, DOI: 10.7939/R3BK1734C.

- Fedotov P.S., Ermolin M.S., Karandashev V.K., and Ladonin D.V. (2014). Characterization of size, morphology and elemental composition of nano-, submicron, and micron particles of street dust separated using field-flow fractionation in a rotating coiled column. *Talanta*, 130, 1–7, DOI: 10.1016/j.talanta.2014.06.040.
- FIRMS (2024). NASA's Fire Information for Resource Management System. [online] Available at: <https://firms.modaps.eosdis.nasa.gov/> [Accessed 2 May 2024].
- Global Coal Plant Tracker (2024). Global Energy Monitor. [online] Available at: <https://globalenergymonitor.org/projects/global-coal-plant-tracker/tracker/> [Accessed 12 July 2024].
- Grigoratos T. and Martini G. (2015). Brake wear particle emissions: a review. *Environmental Science and Pollution Research*, 22 (4), 2491–2504, DOI: 10.1007/s11356-014-3696-8.
- Grivas G., Cheristanidis S., Chaloulakou A., Koutrakis P., and Mihalopoulos N. (2018). Elemental composition and source apportionment of fine and coarse particles at traffic and urban background locations in Athens, Greece. *Aerosol and Air Quality Research*, 18 (7), 1642–1659, DOI: 10.4209/aaqr.2017.12.0567.
- Gubanova D.P., Iordanskii M.A., Kuderina T.M., Skorokhod A.I., Elansky N.F., and Minashkin V.M. (2021). Elemental composition of aerosols in the near-surface air of Moscow: Seasonal changes in 2019 and 2020. *Atmospheric and Oceanic Optics*, 34 (5), 475–482, DOI: 10.1134/S1024856021050122.
- Gunawardana C., Goonetilleke A., Egodawatta P., Dawes L., and Kokot S. (2012). Source characterisation of road dust based on chemical and mineralogical composition. *Chemosphere*, 87 (2), 163–170, DOI: 10.1016/j.chemosphere.2011.12.012.
- Guo J., Kang S., Huang J., Zhang Q., Tripathi L., and Sillanpää M. (2014). Seasonal variations of trace elements in precipitation at the largest city in Tibet, Lhasa. *Atmospheric Research*, 153, 87–97, DOI: 10.1016/j.atmosres.2014.07.030.
- Harrison R.M., Jones A.M., Gietl J., Yin J., and Green D.C. (2012). Estimation of the contributions of brake dust, tire wear, and resuspension to nonexhaust traffic particles derived from atmospheric measurements. *Environmental Science & Technology*, 46 (12), 6523–6529, DOI: 10.1021/es300894r.
- Hulskotte J.H.J., Roskam G.D., and Denier van der Gon H.A.C. (2014). Elemental composition of current automotive braking materials and derived air emission factors. *Atmospheric Environment*, 99, 436–445, DOI: 10.1016/j.atmosenv.2014.10.007.
- Ivanev A.I., Brzhezinskiy A.S., Karandashev V.K., Ermolin M.S., and Fedotov P.S. (2023). Assessment of sources, environmental, ecological, and health risks of potentially toxic elements in urban dust of Moscow megacity, Russia. *Chemosphere*, 321, 138142, DOI: 10.1016/j.chemosphere.2023.138142.
- Jain S., Sharma S.K., Mandal T.K., and Saxena M. (2018). Source apportionment of PM10 in Delhi, India using PCA/APCS, UNMIX and PMF. *Particuology*, 37, 107–118, DOI: 10.1016/j.partic.2017.05.009.
- Kasimov N., Chalov S., Chubarova N., Kosheleva N., Popovicheva O., Shartova N., Stepanenko V., Androsova E., Chichayeva M., Erina O., Kirsanov A., Kovach R., Revich B., Shinkareva G., Tereshina M., Varentsov M., Vasil'chuk J., Vlasov D., Denisova I., and Minkina T. (2024). Urban heat and pollution island in the Moscow megacity: Urban environmental compartments and their interactions. *Urban Climate*, 55, 101972, DOI: 10.1016/j.uclim.2024.101972.
- Kasimov N.S., Kosheleva N.E., Popovicheva O.B., Vlasov D.V., Shinkareva G.L., Erina O.N., Chalov S.R., Chichayeva M.A., Kovach R.G., Zavgorodnyaya Yu.A., and Lychagin M.Yu. (2023). Moscow megacity pollution: Monitoring of chemical composition of microparticles in the Atmosphere–Snow–Road Dust–Soil–Surface Water system. *Russian Meteorology and Hydrology*, 48 (5), 391–401, DOI: 10.3103/S1068373923050011.
- Kasimov N.S., Kosheleva N.E., Vlasov D.V., Nabelkina K.S., and Ryzhov A.V. (2019). Physicochemical properties of road dust in Moscow. *Geography, Environment, Sustainability*, 12 (4), 96–113, DOI: 10.24057/2071-9388-2019-55.
- Kasimov N.S., Vlasov D.V., and Kosheleva N.E. (2020). Enrichment of road dust particles and adjacent environments with metals and metalloids in eastern Moscow. *Urban Climate*, 32, 100638, DOI: 10.1016/j.uclim.2020.100638.
- Kolesnikova V.M., Salimgareeva O.A., Ladonin D.V., Vertyankina V.Y., and Shelegina A.S. (2023). Morphological and mineralogical characteristics of atmospheric microparticles and chemical pollution of street dust in the Moscow Region. *Atmosphere*, 14 (2), 403, DOI: 10.3390/atmos14020403.
- Konstantinova E., Minkina T., Konstantinov A., Sushkova S., Antonenko E., Kurasova A., and Loiko S. (2022). Pollution status and human health risk assessment of potentially toxic elements and polycyclic aromatic hydrocarbons in urban street dust of Tyumen city, Russia. *Environmental Geochemistry and Health*, 44, 409–432, DOI: 10.1007/s10653-020-00692-2.
- Konstantinova E., Minkina T., Nevidomskaya D., Lychagin M., Bezberdaya L., Burachevskaya M., Rajput V.D., Zamulina I., Bauer T., and Mandzhieva S. (2024). Potentially toxic elements in urban soils of the coastal city of the Sea of Azov: Levels, sources, pollution and risk assessment. *Environmental Research*, 252, 119080, DOI: 10.1016/j.envres.2024.119080.
- Kosheleva N.E., Kasimov N.S., and Vlasov D.V. (2015). Factors of the accumulation of heavy metals and metalloids at geochemical barriers in urban soils. *Eurasian Soil Science*, 48 (5), 476–492, DOI: 10.1134/S1064229315050038.
- Kosheleva N.E., Vlasov D.V., Korlyakov I.D., and Kasimov N.S. (2018). Contamination of urban soils with heavy metals in Moscow as affected by building development. *Science of The Total Environment*, 636, 854–863, DOI: 10.1016/j.scitotenv.2018.04.308.
- Kosheleva N.E., Vlasov D.V., Timofeev I.V., Samsonov T.E., and Kasimov N.S. (2023). Benzo[a]pyrene in Moscow road dust: pollution levels and health risks. *Environmental Geochemistry and Health*, 45, 1669–1694, DOI: 10.1007/s10653-022-01287-9.
- Kumar S., Aggarwal S.G., Gupta P.K., and Kawamura K. (2015). Investigation of the tracers for plastic-enriched waste burning aerosols. *Atmospheric Environment*, 108, 49–58, DOI: 10.1016/j.atmosenv.2015.02.066.
- Ladonin D.V. and Mikhaylova A.P. (2020). Heavy metals and arsenic in soils and street dust of the Southeastern Administrative District of Moscow: Long-term data. *Eurasian Soil Science*, 53 (11), 1635–1644, DOI: 10.1134/S1064229320110095.
- Ma C.-J. and Kang G.-U. (2018). Particle scavenging properties of rain clarified by a complementary study with bulk and semi-bulk samples. *Journal of Korean Society for Atmospheric Environment*, 34 (1), 177–186, DOI: 10.5572/KOSAE.2018.34.1.177.
- Meng Y., Li R., Cui L., Wang Z., and Fu H. (2022). Phosphorus emission from open burning of major crop residues in China. *Chemosphere*, 288, 132568, DOI: 10.1016/j.chemosphere.2021.132568.
- Morera-Gómez Y., Alonso-Hernández C.M., Santamaría J.M., Elustondo D., Lasheras E., and Widory D. (2020). Levels, spatial distribution, risk assessment, and sources of environmental contamination vectored by road dust in Cienfuegos (Cuba) revealed by chemical and C and N stable isotope compositions. *Environmental Science and Pollution Research*, 27 (2), 2184–2196, DOI: 10.1007/s11356-019-06783-7.
- Moskovchenko D., Pozhitkov R., and Ukarkhanova D. (2022). Geochemistry of street dust in Tyumen, Russia: influence of traffic load. *Environmental Science and Pollution Research*, 29, 31180–31197, DOI: 10.1007/s11356-021-18013-0.
- Niyobuhungiro R.V. and Blottnitz H. von (2013). Investigation of arsenic airborne in particulate matter around caterers' wood fires in the Cape Town region. *Aerosol and Air Quality Research*, 13 (1), 219–224, DOI: 10.4209/aaqr.2012.06.0148.

- NSAM № 520 AES/MS (2017). Determination of the elemental composition of natural, drinking, sewage and sea waters by atomic emission and mass spectral methods with inductively coupled plasma. Moscow, Russia.
- Orlović-Leko P., Vidović K., Ciglencečki I., Omanović D., Sikirić M.D., and Šimunić I. (2020). Physico-chemical characterization of an urban rainwater (Zagreb, Croatia). *Atmosphere*, 11 (2), 144, DOI: 10.3390/atmos11020144.
- Ozaki H., Yoshimura K., Asaoka Y., and Hayashi S. (2021). Antimony from brake dust to the combined sewer collection system via road effluent under rainy conditions. *Environmental Monitoring and Assessment*, 193 (6), 369, DOI: 10.1007/s10661-021-09152-5.
- Özsoy T. and Örnektekin S. (2009). Trace elements in urban and suburban rainfall, Mersin, Northeastern Mediterranean. *Atmospheric Research*, 94 (2), 203–219, DOI: 10.1016/j.atmosres.2009.05.017.
- Padoan E., Malandrino M., Giacomino A., Grosa M.M., Lollobrigida F., Martini S., and Abollino O. (2016). Spatial distribution and potential sources of trace elements in PM10 monitored in urban and rural sites of Piedmont Region. *Chemosphere*, 145, 495–507, DOI: 10.1016/j.chemosphere.2015.11.094.
- Pant P. and Harrison R.M. (2013). Estimation of the contribution of road traffic emissions to particulate matter concentrations from field measurements: A review. *Atmospheric Environment*, 77, 78–97, DOI: 10.1016/j.atmosenv.2013.04.028.
- Park S.-M., Seo B.-K., Lee G., Kahng S.-H., and Jang Y. (2015). Chemical composition of water soluble inorganic species in precipitation at Shihwa basin, Korea. *Atmosphere*, 6 (6), 732–750, DOI: 10.3390/atmos6060732.
- Polyakova O.V., Artaev V.B., and Lebedev A.T. (2018). Priority and emerging pollutants in the Moscow rain. *Science of The Total Environment*, 645, 1126–1134, DOI: 10.1016/j.scitotenv.2018.07.215.
- Popovicheva O., Diapouli E., Chichayeva M., Kosheleva N., Kovach R., Bitukova V., Eleftheriadis K., and Kasimov N. (2024). Aerosol characterization and peculiarities of source apportionment in Moscow, the largest and northernmost European megacity. *Science of The Total Environment*, 918, 170315, DOI: 10.1016/j.scitotenv.2024.170315.
- Popovicheva O.B., Volpert E., Sitnikov N.M., Chichayeva M.A., and Padoan S. (2020). Black carbon in spring aerosols of Moscow urban background. *Geography, Environment, Sustainability*, 13 (1), 233–243, DOI: 10.24057/2071-9388-2019-90.
- Ramírez O., Sánchez de la Campa A.M., Amato F., Moreno T., Silva L.F., and de la Rosa J.D. (2019). Physicochemical characterization and sources of the thoracic fraction of road dust in a Latin American megacity. *Science of The Total Environment*, 652, 434–446, DOI: 10.1016/j.scitotenv.2018.10.214.
- Rathore D.S., Singh P., Misra C.D., Chandel C.P.S., Bugalia S., and Gupta K.S. (2023). Heavy and less common metals in rainwater and the kinetics of the oxidation of hydrogen sulfide by oxygen in rainwater medium. *Environmental Monitoring and Assessment*, 195 (6), 762, DOI: 10.1007/s10661-023-11374-8.
- Rolph G., Stein A., and Stunder B. (2017). Real-time Environmental Applications and Display sYstem: READY. *Environmental Modelling & Software*, 95, 210–228, DOI: 10.1016/j.envsoft.2017.06.025.
- Romzaykina O.N., Vasenev V.I., Paltseva A., Kuzyakov Y.V., Neaman A., and Dovletyarova E.A. (2021). Assessing and mapping urban soils as geochemical barriers for contamination by heavy metal(loid)s in Moscow megapolis. *Journal of Environmental Quality*, 50, 22–37, DOI: 10.1002/jeq2.20142.
- Rudnick R.L. and Gao S. (2014). Composition of the Continental Crust, in *Treatise on Geochemistry*, Elsevier, pp. 1–51.
- Seinfeld J.H. and Pandis S.N. (2016). *Atmospheric Chemistry and Physics: From Air Pollution to Climate Change*, Third Edition. ed. Hoboken, New Jersey, USA: John Wiley & Sons.
- Semenets E.S., Svistov P.F., and Talash A.S. (2017). Chemical composition of atmospheric precipitation in Russian Subarctic. *Bulletin of the Tomsk Polytechnic University. Geo Assets Engineering*, 328 (3), 27–36.
- Serdyukova A.D., Vlasov D.V., Popovicheva O.B., Kosheleva N.E., Chichayeva M.A., and Kasimov N.S. (2023). Elemental composition of atmospheric PM10 during COVID-19 lockdown and recovery periods in Moscow (April–July 2020). *Environmental Geochemistry and Health*, 45, 7909–7931, DOI: 10.1007/s10653-023-01698-2.
- Song F. and Gao Y. (2009). Chemical characteristics of precipitation at metropolitan Newark in the US East Coast. *Atmospheric Environment*, 43 (32), 4903–4913, DOI: 10.1016/j.atmosenv.2009.07.024.
- Stein A.F., Draxler R.R., Rolph G.D., Stunder B.J.B., Cohen M.D., and Ngan F. (2015). NOAA's HYSPLIT Atmospheric Transport and Dispersion Modeling System. *Bulletin of the American Meteorological Society*, 96 (12), 2059–2077, DOI: 10.1175/BAMS-D-14-00110.1.
- Stepanets V.N., Malygina N.S., Lovtskaya O.V., and Papina T.S. (2021). Regional-scale impacts of the major tin plant on the chemical composition of atmospheric precipitation in the south of Western Siberia (Russia). *Environmental Earth Sciences*, 80 (20), 701, DOI: 10.1007/s12665-021-09970-3.
- Tsamos P., Koliass P., Lambropoulou D., and Noli F. (2022). Distribution and temporal variability of uranium and toxic metal(loid)s in snow and rainwater from an oil industry and urban area in Thessaloniki-Greece. *Science of The Total Environment*, 838, 155604, DOI: 10.1016/j.scitotenv.2022.155604.
- Vetrova A.A., Sazonova O.I., Ivanova A.A., Streletskii R.A., Sarzhanov D.A., Korneykova M.V., Novikov A.I., Vasenev V.I., Ivashchenko K.V., Slukovskaya M.V., and Gavrichkova O. (2023). Diversity of microbial communities, PAHs, and metals in road and leaf dust of functional zones of Moscow and Murmansk. *Microorganisms*, 11 (2), 526, DOI: 10.3390/microorganisms11020526.
- Vlasov D.V., Eremina I.D., Shinkareva G.L., Chubarova N.E., and Kasimov N.S. (2021a). Daily variations in wet deposition and washout rates of potentially toxic elements in Moscow during spring season. *Geography, Environment, Sustainability*, 14 (1), 219–233, DOI: 10.24057/2071-9388-2020-162.
- Vlasov D.V., Kasimov N., Eremina I., Shinkareva G., and Chubarova N. (2021b). Partitioning and solubilities of metals and metalloids in spring rains in Moscow megacity. *Atmospheric Pollution Research*, 12 (1), 255–271, DOI: 10.1016/j.apr.2020.09.012.
- Vlasov D.V., Kosheleva N., and Kasimov N. (2021c). Spatial distribution and sources of potentially toxic elements in road dust and its PM10 fraction of Moscow megacity. *Science of The Total Environment*, 761, 143267, DOI: 10.1016/j.scitotenv.2020.143267.
- Vlasov D.V., Kukushkina O.V., Kosheleva N.E., and Kasimov N.S. (2022). Levels and factors of the accumulation of metals and metalloids in roadside soils, road dust and their PM10 fraction in the Western Okrug of Moscow. *Eurasian Soil Science*, 55 (5), 556–572, DOI: 10.1134/S1064229322050118.
- Vlasov D.V., Kasimov N., Eremina I., Shinkareva G., and Chubarova N. (2023a). Major ions and potentially toxic elements in atmospheric precipitation during the COVID-19 lockdown in Moscow megacity. *Urban Climate*, 48, 101422, DOI: 10.1016/j.uclim.2023.101422.
- Vlasov D.V., Vasil'chuk J.Yu., Kosheleva N.E., and Kasimov N.S. (2023b). Contamination levels and source apportionment of potentially toxic elements in size-fractionated road dust of Moscow. *Environmental Science and Pollution Research*, 30 (13), 38099–38120, DOI: 10.1007/s11356-022-24934-1.
- von Gunten K., Konhauser K.O., and Alessi D.S. (2020). Potential of asphalt concrete as a source of trace metals. *Environmental Geochemistry and Health*, 42 (2), 397–405, DOI: 10.1007/s10653-019-00370-y.

Wada K., Simpson R., Kishimoto N., and Takei N. (2020). Motor vehicle wash-off water as a source of phosphorus in roadway runoff. *Journal of Water and Environment Technology*, 18 (1), 9–16, DOI: 10.2965/jwet.19-047.

Xu Y., Li Q., Xie S., Zhang C., Yan F., Liu Y., Kang S., Gao S., and Li C. (2022). Overestimation of anthropogenic contribution of heavy metals in precipitation than those of aerosol samples due to different treatment methods. *Environmental Pollution*, 300, 118956, DOI: 10.1016/j.envpol.2022.118956.

Yanchenko N.I. and Yaskina O.L. (2014). Features of chemical composition of snow cover and precipitation in Bratsk. *Bulletin of the Tomsk Polytechnic University. Geo Assets Engineering*, 324, 27–35.

Yang X., Wang X., Zhang Y., Lee J., Su J., and Gates R.S. (2011). Characterization of trace elements and ions in PM10 and PM2.5 emitted from animal confinement buildings. *Atmospheric Environment*, 45 (39), 7096–7104, DOI: 10.1016/j.atmosenv.2011.09.037.

Zappi A., Popovicheva O., Tositti L., Chichaeva M., Eremina I., Kasper-Giebl A., Tsai Y.I., Vlasov D., and Kasimov N. (2023). Factors influencing aerosol and precipitation ion chemistry in urban background of Moscow megacity. *Atmospheric Environment*, 294, 119458, DOI: 10.1016/j.atmosenv.2022.119458.

Zeng J., Yue F.-J., Li S.-L., Wang Z.-J., Wu Q., Qin C.-Q., and Yan Z.-L. (2020). Determining rainwater chemistry to reveal alkaline rain trend in Southwest China: Evidence from a frequent-rainy karst area with extensive agricultural production. *Environmental Pollution*, 266, 115166, DOI: 10.1016/j.envpol.2020.115166.

Zeng J., Han G., Wu Q., Peng M., Ge X., Mao S., Wang Z.-J., and Ma Q. (2024a). Chemical evolution of rainfall in China's first eco-civilization demonstration city: Implication for the provenance identification of pollutants and rainwater acid neutralization. *Science of The Total Environment*, 910, 168567, DOI: 10.1016/j.scitotenv.2023.168567.

Zeng J., Han G., Zhang S., Zhang Q., and Qu R. (2024b). Potentially toxic elements in rainwater during extreme rainfall period in the megacity Beijing: Variations, sources, and reuse potential. *Atmospheric Environment*, 318, 120242, DOI: 10.1016/j.atmosenv.2023.120242.

Zheng J., Zhan C., Yao R., Zhang J., Liu H., Liu T., Xiao W., Liu X., and Cao J. (2018). Levels, sources, markers and health risks of heavy metals in PM2.5 over a typical mining and metallurgical city of Central China. *Aerosol Science and Engineering*, 2 (1), 1–10, DOI: 10.1007/s41810-017-0018-9.